Journal of Alloys and Compounds 317–318 (2001) 350–356

Journal of ALLOYS AND COMPOUNDS

www.elsevier.com/locate/jallcom

Phase equilibria and magnetic studies in the ternary system Ce–Au–Sn

P. Boulet[a,b,c,*], D. Mazzone[b], H. Noël[a], P. Rogl[c], R. Ferro[b]

[a] *Laboratoire de Chimie du Solide et Inorganique Moléculaire, U.M.R. C.N.R.S 6511, Université de Rennes 1, Avenue du Général Leclerc – 35042 Rennes, France*

[b] *Dipartimento di Chimica e Chimica Industriale – Università di Genova Via Dodecaneso, 31-16146 Genova, Italy*

[c] *Institut für Physikalische Chemie der Universität Wien, A-1090 Wien, Währingerstraße 42, Austria*

Abstract

The phase equilibria in the ternary system Ce–Au–Sn have been established in an isothermal section at 750°C. Experimental techniques used were optical microscopy, EPMA and X-ray powder analysis of arc-melted samples which were annealed at 750°C for 10 days and quenched to room temperature. Phase equilibria are characterized by the formation of seven ternary phases, of which only the equiatomic compound CeAuSn ($CaIn_2$-type) was already reported. Their crystal structures and physical properties were investigated and are presented.

Keywords: Ternary phase diagram; Intermetallics; Magnetic properties

1. Introduction

Since many years ago, important research activities have been devoted to uranium and rare-earth intermetallic compounds because of their interesting physical properties comprising long range magnetic order, enhanced Pauli paramagnetism, heavy fermion ground states, intermediate valence states or even superconductivity. The physical properties of these compounds are mainly governed by the strength of the f-(spd) hybridization, i.e. the interaction of the f electrons with the conduction electrons. However, in some cases conflicting results were reported on the same compound due to the fact that physical properties are very sensitive to the history of the sample like heat treatment, homogeneity domain or presence of impurities. To know the intrinsic physical properties of these compounds the first step is to determine their relation of equilibrium with the neighbouring phases and to evaluate their homogeneity range. We recently reported the results obtained in the Ce–Ag–Sn [1], U–Ag–Sn [2] and U–Au–Sn [3] isothermal sections at 750°C. The subject of the present paper consists of the complete investigation of the system Ce–Au–Sn at 750°C by means of X-ray diffraction, EPMA and magnetic susceptibility measurements of the ternary phases observed.

2. Experimental details

Polycrystalline ingots were obtained by arc melting stoichiometric amounts of the constituent elements under an atmosphere of high purity argon on a water-cooled copper hearth, using a Ti–Zr alloy as an oxygen getter. The materials were used in the form of ingots as supplied by Merck AG (cerium 99.8% pure, gold 3 N) and by Strem Chemicals (tin 2 N8). In order to ensure homogeneity, the arc melted button was turned over and remelted three times, with weight losses lower than 0.5%. To improve the quality of the crystallites, the arc-melted buttons were wrapped in tantalum foil, sealed in an evacuated quartz tube, annealed at 750°C for 10 days and quenched by submerging in water. Precise lattice parameters and standard deviations were obtained by least squares refinement of X-ray powder diffraction data (monochromated Cu $K\alpha_1$ radiation) collected on an INEL CPS 120 diffractometer equipped with a position-sensitive detector covering 120° in 2θ, and using silicon as internal standard. Alloys of cerium with tin are known to be highly moisture sensitive and pyrophoric, therefore they were handled in a glove-box under an inert argon atmosphere, ensuring an oxygen level

---

*Corresponding author. Present address: Institut for Transuranium Elements, ITU, Postfach 2340, D-76125 Karlsruhe, Germany.

E-mail address: boulet@itu.fzk.de (P. Boulet).

0925-8388/01/$ – see front matter
PII: S0925-8388(00)01429-8

of less than 3 ppm O_2 and about 2 ppm H_2O. Metallographic examination was carried out using optical and scanning electron microscopy. Semiquantitative microanalysis of the phases was performed using an EDS microanalyzer.

Magnetic measurements were performed on annealed polycrystalline sample using a SQUID (SHE) magnetometer in the temperature range 2–300 K and in the magnetic field range 0–3 T.

3. Results and discussion

3.1. The binary boundary systems

The binary boundary systems were essentially accepted in the version published in Massalski [4], except for the system Ce–Sn, which was recently reinvestigated [5–7].

Concerning the Ce–Au binary phase diagram, we confirm the existence of the binary phases with the crystal structures reported in the literature [4,8]. All these phases were found to dissolve various amounts of tin ranging from 9% for CeAu (FeB-type) and $CeAu_2$ ($CeCu_2$-type) to 7% for $Ce_{14}Au_{51}$ ($Gd_{14}Ag_{51}$-type), respectively. According to the diagram reported in the literature [4] the phase Ce_2Au (Co_2Si-type) was not observed during this work since it was reported to form below 665°C. Moreover the phase $CeAu_6$ ($PrAu_6$-type), reported as a dashed line and formed peritectically above 800°C, was not observed during our investigation neither in the samples prepared in the ternary system nor in the binary itself. This would suggest that this phase forms at a temperature lower than 750°C.

As observed during the investigation of the Ce–Ag–Sn [1] ternary system, performed at the same temperature, the Ce–Sn binary phases were found to dissolve various amounts of transition metals. For the Ce–Au–Sn system gold solubility at 750°C was found to reach 10% in $CeSn_3$ ($AuCu_3$-type), 5% in Ce_3Sn_5 (Pu_3Pd_5-type) and 4% in Ce_5Sn_4 (Sm_5Ge_4-type) and Ce_5Sn_3 (W_5Si_3-type).

3.2. Isothermal section of Ce–Au–Sn at 750°C

Fig. 1 summarizes the results obtained from the examination of several alloys in the complete composition range. The isothermal section can be described in three different parts.

The first part, lying near the Au–Sn binary system [4] and in agreement with it, shows a large liquid domain which is represented by dashed lines since its border could not be determined by our experimental procedure.

The second part, near the cerium rich region, is also in equilibrium with the liquid since both corresponding binary phase diagrams Ce–Au and Ce–Sn show a eutectic transformation near Ce, at a temperature lower than 750°C. It should be noted that the samples in this region were found to be very oxidizable like Ce–Sn binary compounds.

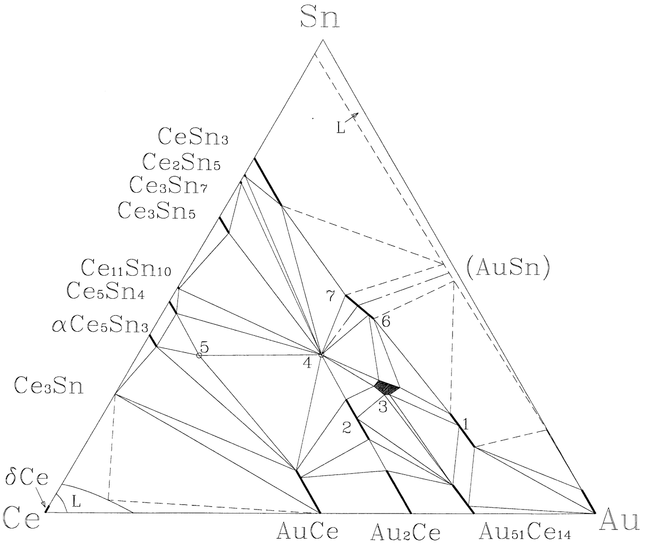

Fig. 1. Isothermal section at 750°C of the Ce–Au–Sn system.

The last part of this isothermal section lies in the middle of the system, and shows the existence of seven individual ternary phases, which will be described below.

Only the equiatomic phase CeAuSn (hexagonal, $CaIn_2$-type) [9] was reported in this system. Microprobe analysis and XRD measurement allowed us to detect at least six new ternary phases. Their crystallographic data are reported in Table 1.

3.3. Crystallographic properties of the ternary phases

3.3.1. Phase n. 1: $CeAu_5Sn$–$Ce_3Au_{13}Sn_4$

Recently some compounds with this composition range were reported in various ternary systems but only a few of their crystallographic structures were given: $Ce_2Cu_9Sn_{2.65}$ and $CeCu_5Sn$ [10,11] both related to the $CeCu_6$ structure type, $Ce_{16}Pd_{60}Ge_{24}$ [12] (unknown structure), $Pr_{15}Cu_{65}Sn_{20}$ and $Lu_{12.5}Cu_{67.5}Sn_{20}$ [13] (unknown structure), $CeNi_5Sn$ [14] which crystallizes with a hexagonal structure, and $U_3Au_{13}Al_4$ [15]. This phase was found in the Ce–Au–Sn system by electron microprobe measurements with an homogeneity ranging from the $CeAu_5Sn$ to the $Ce_3Au_{13}Sn_4$ compositions, corresponding to a general formula $Ce_3Au_{15\pm x}Sn_{3\pm y}$, with $0<x<2$ and $0<y<1$. The X-ray powder patterns of the samples prepared along this solid solution were found to be identical with only a small change in intensity and confirmed the existence of a solid solution. As we observed for $U_3Au_{13}Al_4$, it crystallizes with a body-centered cubic unit cell, with $a=15.12$ Å for the composition $Ce_3Au_{13}Sn_4$ and $a=15.09$ Å for $CeAu_5Sn$. Single crystals of this phase were easily found in the arc-melted sample and the X-ray diffraction data were collected on a Nonius CAD-4 four circle diffractometer. Their experimental conditions are reported in Table 2.

Table 1
Crystallographic data for ternary compounds in the system Ce–Au–Sn

Phase	Space group, Pearson symbol and prototype	Lattice parameters (Å)	
		This work	Literature
1 – CeAu$_5$Sn to Ce$_3$Au$_{13}$Sn$_4$	I 23, cI168-filled Be$_{17}$Ru$_3$-type	$a=15.096(2)$ $a=15.127(3)$	
2 – CeAu$_{2-x}$Sn$_x$	Hexagonal, intergrowth of AlB$_2$-type	$a=8.313(1)$ $c=9.528(3)$	
3 – CeAu$_2$Sn	Hexagonal, hP16, superstructure of the ZrPt$_2$Al-type	$a=9.517(1)$ $c=9.591(3)$	
4 – CeAuSn	$P6_3/mmc$ hP6 – CaIn$_2$-type	$a=4.731(2)$ $c=7.712(3)$	$a=4.73$ $c=7.71$ [8,9]
5 – Ce$_5$AuSn$_3$	$P6_3/mcm$ hP18 – Hf$_5$CuSn$_3$-type	$a=9.645(5)$ $c=6.754(4)$	
6 – CeAu$_2$Sn$_2$	Orthorhombic, superstructure of the ThCr$_2$Si$_2$-type	$a=4.575(1)$ $b=13.590(1)$ $c=10.176(1)$	
7 – Ce$_2$Au$_3$Sn$_4$	Tetragonal, superstructure of the ThCr$_2$Si$_2$-type	$a=9.142(2)$ $c=10.359(3)$	

The data processing was carried out on a VAX 3100 computer using the MOLEN Package [16]. The lattice parameter determined from least squares analysis of the setting angle of 25 X-ray reflections has the value $a=15.118(1)$ Å. The X-ray diffraction intensities were corrected for Lorentz and polarization effects and an absorption correction was applied using the Psiscan program. The inspection of the systematic extinctions revealed no other extinction than those due to the body centering. The structure was successfully refined in the space group $I23$ (n°197). The positions of the gold and cerium atoms were derived using direct methods (Multan program) and the positions of the tin atoms were obtained from subsequent difference Fourier calculations. Several cycles of refinement of the positional and isotropic displacement parameters converged to the agreement factors $R=0.075$ and $R_w=0.085$. Owing to the large isotropic displacement parameters of some atoms, their occupation factors were successively refined revealing some defect on Au(1) and Sn(3) sites, leading to the reliability factor $R=0.070$ and $R_w=0.081$. Final refinements carried out including the anisotropic factor of all the atomic sites lead to the final residual values of $R=0.053$ and $R_w=0.060$. Thus, the composition of the investigated single crystal is Ce$_3$Au$_{14.2}$Sn$_{2.7}$. It should be mentioned that a non-negligible electron density was observed in different fourier maps in a 8c position, that was attributed to the tin atom Sn(3) although the refinements led to a low occupation and a very large thermal factor, indicating a highly delocalized atom.

Table 2
Crystallographic data for Ce$_3$Au$_{14.2}$Sn$_{2.7}$

Formula	Ce$_3$Au$_{14.2}$Sn$_{3.2}$
Space group	$I23$. n°197
Crystal dimensions (mm)	$0.04\times0.06\times0.06$
Linear absorption coefficient (cm^{-1})	1387.2
Lattice parameter (from CAD4)	15.118(1) Å
Unit-cell volume (Å^3)	3455.3(1)
Calculated density (g cm^{-3})	14.34
Formula per unit cell	$Z=8$
Formula weight (g)	3557.6
Scan range	$1<\theta<35°$
	$0<h<24$
	$0<k<24$
	$0<l<24$
Total observed reflections	3916
Independent reflections with $I>3\sigma(I)$	455
Secondary extinction coefficient	$g=5.78\times10^{-9}$ corr.$=1/(1+gI_c)$
Number of variables	66
Reliability factors:	
$R=\Sigma\ [\lvert F_o\rvert-\lvert F_c\rvert]/\Sigma\ \lvert F_o\rvert$	0.053
$R_w=[\Sigma_w\ (\lvert F_o\rvert-\lvert F_c\rvert)^2/\Sigma_w\ \lvert F_o\rvert^2]^{1/2}$	0.059
Goodness of fit GOF	1.07

A search for parent compounds from a database of inorganic compounds revealed that this compound is similar to those listed below but resolved in the centrosymmetric space group Im-3 (n°204): Be$_{17}$Ru$_3$ [17], Cd$_6$Yb [18] and Cd$_6$Y [19]. The refinement in the centrosymmetric space group Im-3 did not succeed for our compound, but after normalization of the atomic position of the structures mentioned above into the space group $I23$, the following comment can be made:

- The Be$_{17}$Ru$_3$ structure corresponds to the same arrangement where the atomic site 8c of Sn(3) is not occupied.
- Cd$_6$Y corresponds to the filled Be$_{17}$Ru$_3$-type where there is evidence of one more 24f atomic site, 1/3 of which is occupied by a cadmium atom.
- Cd$_6$Yb is derived from the Be$_{17}$Ru$_3$-type but with two more 8c atomic sites, 1/2 of which is occupied by a cadmium atom.

All these structures were checked and did not lead to a better result, and it is worth mentioning here that the

Table 3
Atomic parameters for $Ce_3Au_{14.2}Sn_{2.7}$

Atom	Site	x	y	z	Occ.	B_{eq} (Å^2)
Au(1)	24f	0.0	0.0901(2)	0.2433(3)	0.88	1.29(6)
Ce	24f	0.0	0.3030(3)	0.1878(3)		0.44(6)
Au(2)	24f	0.0943(2)	0.5	0.1526(2)		0.47(4)
Au(3)	24f	0.1110(3)	0.2017(2)	0.3404(2)		0.90(6)
Au(4)	24f	0.1523(3)	0.3931(3)	0.3019(2)		0.98(6)
Sn(1)	12e	0.1878(5)	0.5	0.0		1.0(1)
Au(5)	12d	0.4085(3)	0.0	0.0		1.81(9)
Au(6)	8c	0.1534(3)	–	–		0.83(3)
Sn(2)	8c	0.3514(8)	–	–		2.23(5)
Sn(3)	8c	0.257(3)	–	–	0.22	6.0(1)

isotropic factor reported for these parent compounds were also very large for some atomic sites.

The positional parameters standardized using the Structure Tidy program are shown in Table 3 and the main interatomic distances are reported in Table 4.

3.3.2. Phase n. 2: $CeAu_{2-x}Sn_x$, $0.5<x<0.66$

Microprobe analysis allowed us to isolate a new phase with the approximate composition $Ce_3Au_4Sn_2$ which seems to have an extended region towards the composition Ce_2Au_3Sn, i.e. $CeAu_{2-x}Sn_x$, $0.5<x<0.66$. This phase was also observed during the investigation of the U–Au–Sn system [3]. Although the X-ray powder pattern shows similarities to those obtained for the neigbouring phases like CeAuSn ($CaIn_2$-type), $CeAu_2Sn$ (superstructure of the $ZrPt_2Al$-type) and to the solid solution from binary $CeAu_2$ ($CeCu_2$-type), the phase could not be indexed correctly based on these structure types. As the $CaIn_2$-type, the $ZrPt_2Al$-type and the $CeCu_2$-type are all related to the well-known AlB_2-type structure, the phase might therefore be an intergrowth of the AlB_2-type between these neighbouring structures. The lattice parameter refinement of the single crystal obtained leads to a hexagonal unit cell with $a=8.313(1)$ Å and $c=9.528(3)$ Å. The crystal structure refinement of this phase is underway but like the other phases observed in this system further experiments are needed to improve the quality of the single crystals obtained.

Table 4
Main interatomic distances (Å) for $Ce_3Au_{14.2}Sn_{2.7}$ (e.s.d$<$0.004)

Au(1)	1Au(1)	2.715	Au(4)	1Sn(3)	2.695
	1Au(4)	2.749		1Au(1)	2.749
	1Sn(2)	2.776		1Sn(1)	2.793
	1Au(3)	2.834		1Au(2)	2.888
	1Au(5)	2.851		1Au(2)	2.891
	1Au(6)	2.884		1Au(3)	3.051
	2Ce	3.274		1Au(3)	3.070
	1Ce	3.332		1Sn(2)	3.217
Ce	1Au(3)	3.182	Sn(1)	2Au(2)	2.717
	1Au(4)	3.219		2Au(2)	2.787
	1Au(5)	3.259		2Au(4)	2.793
	1Au(3)	3.262		2Au(3)	2.964
	2Au(1)	3.274		2Au(5)	3.164
	1Au(6)	3.276		2Ce	3.516
	1Au(4)	3.287	Au(5)	1Au(5)	2.750
	1Au(3)	3.307		2Au(1)	2.851
Au(2)	1Sn(1)	2.717		4Au(2)	3.042
	1Sn(1)	2.787		2Sn(1)	3.164
	1Au(2)	2.844		2Ce	3.259
	1Au(4)	2.888	Au(6)	1Sn(3)	2.747
	1Au(4)	2.891		3Au(1)	2.884
	1Au(3)	2.952		3Au(3)	2.947
	1Au(3)	2.969		3Ce	3.276
	2Au(5)	3.042	Sn(2)	1Sn(3)	2.453
	2Ce	3.340		3Au(1)	2.776
Au(3)	1Sn(3)	2.686		3Au(4)	3.217
	1Au(1)	2.834		3Ce	3.307
	1Au(7)	2.947	Sn(3)	1Sn(2)	2.453
	1Au(2)	2.947		3Au(3)	2.686
	1Sn(1)	2.952		3Au(4)	2.695
	1Au(2)	2.964		1Au(7)	2.747
	1Au(4)	2.969		3Ce	3.817
	1Au(4)	3.051			

3.3.3. Phase n. 3: $CeAu_2Sn$

This phase was observed by microprobe analyses to have a homogeneity domain around the composition (25:50:25) corresponding to the correct formula $CeAu_{2+x}Sn_{1-x}$ with $0<x<0.1$, i.e. an exchange of tin by gold. The X-ray powder patterns of the samples prepared around this composition are quite similar to the diffractogram obtained for UAu_2Sn ($ZrPt_2Al$-type) [3] but with the indexed lines (h0l) split to two lines with almost the same intensity, whereas the (h00) and the (hhl) lines remain unaffected. This observation leads to a correct indexation using a double axis a of the hexagonal $ZrPt_2Al$-type unit cell. This result was confirmed by single crystal analysis leading to the primitive hexagonal unit cell with $a=9.517(1)$ Å and $c=9.591(3)$ Å; the refinement of the correct structure needs further investigations.

3.3.4. Phase n. 4: CeAuSn

It is confirmed that this phase exists and microprobe analyses show that it seems to be nearly stoichiometric without any homogeneity range. CeAuSn crystallizes with the hexagonal $CaIn_2$-type structure and the lattice parameters $a=4.731(2)$ Å and $c=7.712(3)$ Å obtained are in good agreement with those reported in the literature [9].

3.3.5. Phase n. 5: Ce_5AuSn_3

As we observed for the Ce–Ag–Sn system, the phase Ce_5AuSn_3 was found to crystallize with the hexagonal Hf_5CuSn_3-type. This is the filled variant of the Mn_5Si_3-type structure, adopted by the Ce_5Sn_3 phase at low temperature, i.e below 750°C. When 10% of Ag or Au is added to this binary phase, their structure is maintained with an increase of the a lattice parameter from $a=9.335$ Å for Ce_5Sn_3 [8] to $a=9.576(3)$ Å for Ce_5AgSn_3 [1] and to $a=9.645(5)$ Å for Ce_5AuSn_3 and a decrease of the c

Table 5
Magnetic properties of the ternary compounds in the system Ce–Au–Sn

Compound	Magnetic properties	μ_{eff} (μ_B)	θ_p (K)	χ_0 (10^{-3} emu mole^{-1})
CeAuSn	AF(4.2 K)	2.61	−37.2	
Ce_5AuSn_3	F(5 K)	2.20	−14.7	1.22
$CeAu_5Sn$	CW	2.60	−21.3	
$CeAu_2Sn_2$	CW	2.46	−12.5	
$Ce_2Au_3Sn_4$	CW	2.58	−23.4	
$CeAu_2Sn$	CW	2.48	−9.0	

lattice parameter from $c=6.81$ Å to $c=6.754(4)$ Å and to $c=6.737(2)$ Å, respectively.

3.3.6. Phases n. 6 and 7: $CeAu_2Sn_2$ and $Ce_2Au_3Sn_4$

Ternary intermetallic compounds with the general formula RM_2X_2, where R is a rare-earth or an actinide element, M a transition metal and X an element as Si, Ge or Sn, have drawn the attention of numerous researchers since some of the compounds belong to the heavy fermion family showing superconductive transitions in some cases such as $CeCu_2Si_2$ [20] or URu_2Si_2 [21]. These compounds usually crystallize with the primitive tetragonal $CaBe_2Ge_2$-type or with the body-centered $ThCr_2Si_2$-type. During the investigation of the Ce–Au–Sn system by microprobe analyses in this concentration range we observed a huge homogeneity domain going from the approximate composition $Ce_2Au_3Sn_4$ to $CeAu_2Sn_2$. Nevertheless the X-ray powder pattern of these two compositions were not exactly the same. Single crystals of these compositions were extracted from the annealed buttons and properly recorded on a Nonius CAD-4 four circle diffractometer, leading to two fairly correlated unit cells and confirming the previous examinations on the XRD powder analyses. Single crystals having the composition $CeAu_2Sn_2$ were found to crystallize with a primitive orthorhombic unit cell with $a=4.575(1)$ Å, $b=13.590(1)$ Å and $c=10.176(1)$ Å whereas those of the composition $Ce_2Au_3Sn_4$ were found to crystallize in a primitive tetragonal unit cell with $a=9.142(2)$ Å and $c=10.359(3)$ Å. Unfortunately, due to the poor quality of these single crystals no successful refinement of the real crystal structure has been performed yet. However, we can observe that their unit cell parameters fairly correlate with each other as well as to the well-known $CaBe_2Ge_2$ or to the $ThCr_2Si_2$-type, by the following relations: (a, 3a, c) for $CeAu_2Sn_2$ and (2a, c) for $Ce_2Au_3Sn_4$.

3.4. Magnetic properties of the ternary phases

Magnetic measurements performed on polycrystalline annealed samples are summarized in Table 5. At high temperature most of these ternary phases, except for Ce_5AuSn_3, revealed trivalent cerium. Fig. 2 shows the result obtained for CeAuSn, which was found to order antiferromagnetically below 4.2 K. In the high temperature region ($T>70$ K), the thermal dependence of the inverse magnetic susceptibility follows the Curie–Weiss law: $\chi = C(T-\theta)$. These results are in good agreement with those already reported in the literature [22] revealing an electronic specific heat coefficient of 270 mJ mol^{-1} K^2.

Fig. 3 represents the measurement performed on Ce_5AuSn_3 revealing ferromagnetic ordering below 5 K. As already pointed out [23,24], this structure type is of

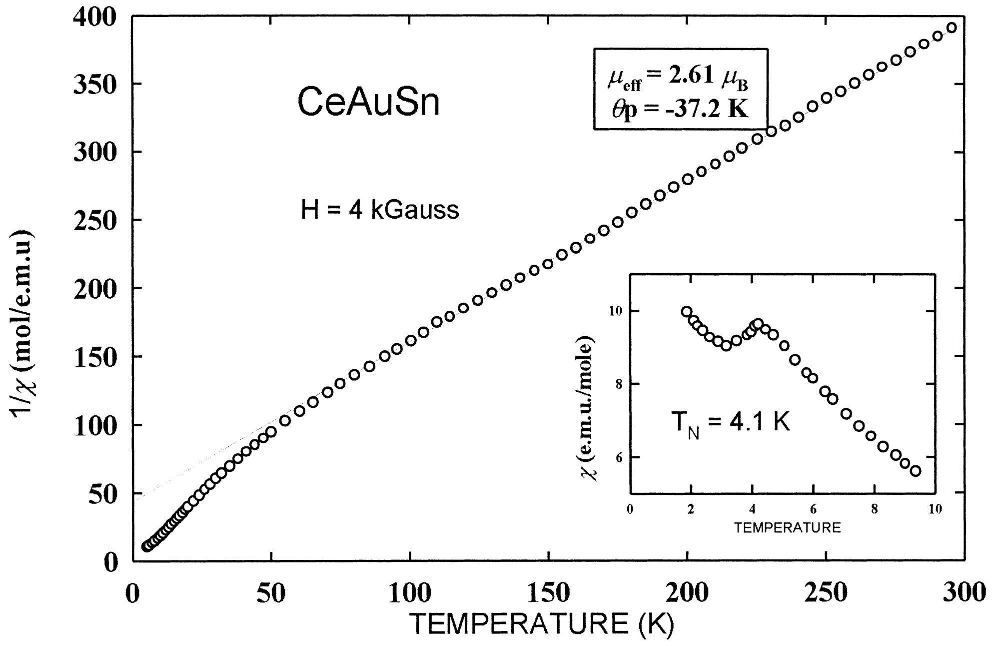

Fig. 2. Temperature dependence of the inverse magnetic susceptibility χ^{-1} of CeAuSn under 4 kG. The symbols represent the measured values and the solid line is a fit by the Curie–Weiss law. The inset shows the susceptibility versus temperature between 2 and 10 K.

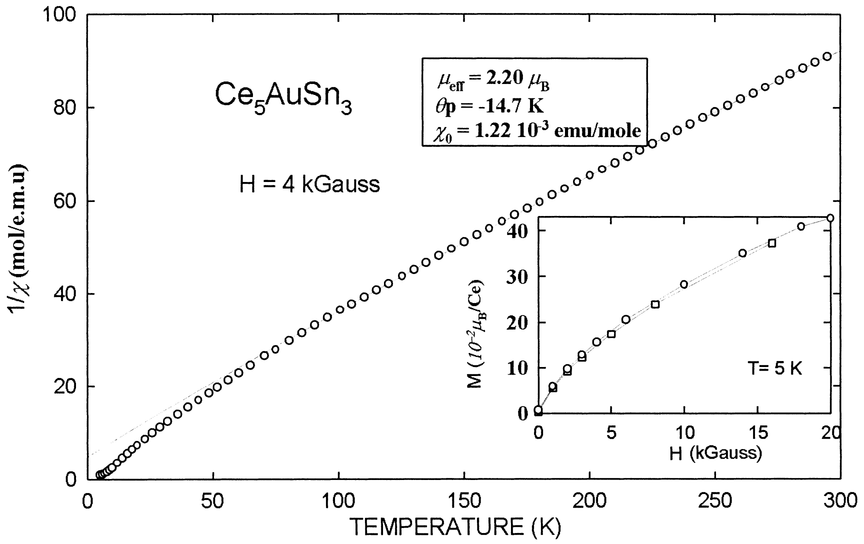

Fig. 3. Temperature dependence of the inverse magnetic susceptibility χ^{-1} of Ce_5AuSn_3 under 4 kG. The symbols represent the measured values and the solid line is a fit by the modified Curie–Weiss law. The inset shows the magnetization versus field at 5 K.

particular interest as it is characterized by the existence of rather short Ce–Ce interatomic distances equal to half of the *c* lattice parameter: $c/2=3.377$ Å for Ce_5AuSn_3. In the paramagnetic state the reciprocal susceptibility of Ce_5AuSn_3 was fitted by a modified Curie–Weiss law, $\chi=\chi_0+C/(T-\theta)$, leading to the paramagnetic values listed in Table 5. The presence of a ferromagnetic order and negative paramagnetic Curie temperature could be explained on the hypothesis of coexistence of ferro- and antiferro-magnetic components in a non-collinear structure as observed for example in the $CePd_2Si$ compounds [25]. The low value of the effective magnetic moment suggests cerium to be in an intermediate valence state, as a result of the existing short distances observed in the cerium sublattices. We can notice that the binary cerium stannide βCe_5Sn_3, which crystallizes in the Mn_5Si_3-type, shows ferromagnetic ordering below $T_C=12$ K [26] with an effective magnetic moment of 2.58 μ_B corresponding to Ce^{3+}. Thus, filling this structure with Au, the cerium environment changes as well as the Ce–Ce interatomic distances which decrease from 3.41 Å in the binary to 3.377 Å in the ternary compound. This decrease probably implies a partial delocalisation of the 4f electrons of cerium, thus leading to a lower effective magnetic moment

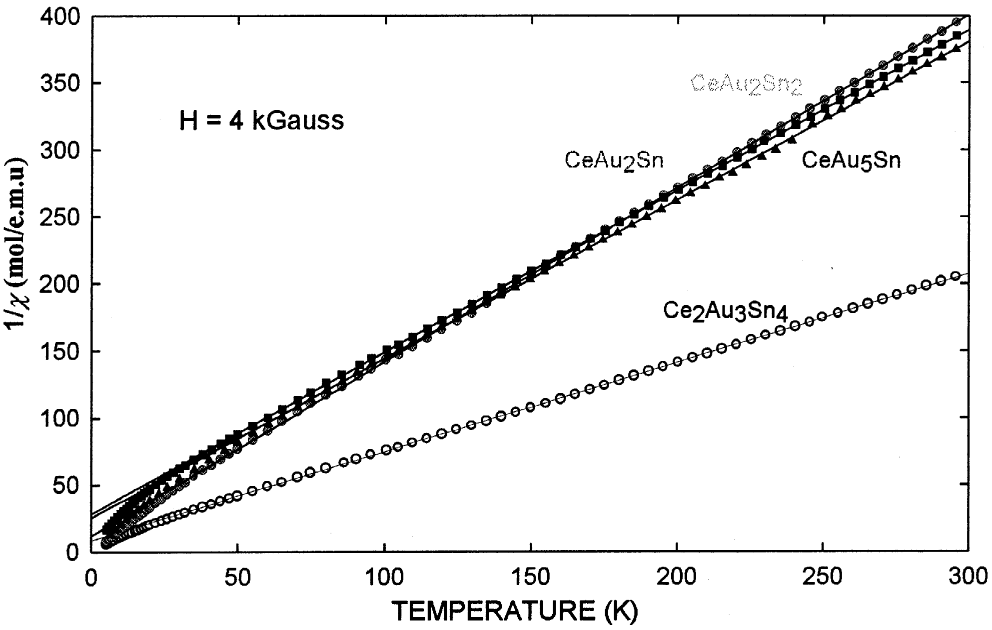

Fig. 4. Temperature dependence of the inverse magnetic susceptibility χ^{-1} of $CeAu_5Sn$, $CeAu_2Sn_2$, $Ce_2Au_3Sn_4$ and $CeAu_2Sn$ under 4 kG. The symbols represent the measured values and the solid lines are a fit by the Curie–Weiss law.

for the ternary Ce_5AuSn_3 than for the parent βCe_5Sn_3 binary compound. It is worth noting that the same behavior was observed for the compound Ce_5AgSn_3 containing silver. Unfortunately no magnetic measurements have ever been reported for the same type of compound containing Cu, whose existence was reported in Ref. [27]. It would be interesting to perform neutron diffraction experiments on these compounds in order to determine the contributions to the magnetic behavior of the different crystallographic sites of the cerium atoms.

The magnetic measurements illustrated in Fig. 4 reveal that no magnetic order is observed above 5 K for the composition $CeAu_5Sn$, $Ce_2Au_3Sn_4$, $CeAu_2Sn_2$ and $CeAu_2Sn$. At high temperature all these compounds follow the Curie–Weiss law.

4. Conclusion

We have investigated the isothermal section of the Ce–Au–Sn ternary system at 750°C which showed the existence of seven ternary phases. In most of the cases these phases seem to have a fairly considerable homogeneity range due to an exchange of Sn by Au at this temperature. Most of these ternary phases are supposed to form congruently or peritectically and further single crystal growth improvements are needed to obtain suitable samples for crystal structure determination. The magnetic measurements of these phases show interesting behaviour going from magnetic order to Curie Weiss behavior above 5 K.

Acknowledgements

This work was supported by the European Community programme: Human Capital and Mobility ERBCHRX – CT93-0284.

References

[1] P. Boulet, D. Mazzone, H. Noël, P. Riani, P. Rogl, R. Ferro, Intermetallics 7 (1999) 931.
[2] P. Boulet, M. Vybornov, A. Simopoulos, A. Kostikas, H. Noël, P. Rogl, J. Alloys Comp. 283 (1–2) (1999) 49.
[3] P. Boulet, M. Vybornov, H. Noël, J. Alloys Comp. 306 (1–2) (2000) 11.
[4] T.B. Massalski, Binary Alloy Phase Diagrams, 2nd Edition, ASM, Metals Park, OH, 1990.
[5] E.A. Franceschi, G.A. Costa, J. Therm. Anal. 34 (1988) 451.
[6] E.A. Franceschi, J. Less-Common Met. 66 (1979) 175.
[7] J.X. Boucherle, F. Givord, P. Lejay, J. Schweizer, A. Stunault, Acta Crystallogr. B 44 (1988) 377.
[8] P. Villars, L.D. Calvert, Pearson's Handbook of Crystallographic Data for Intermetallic Phases, 2nd Edition, ASM International, Materials Park, OH, 1991.
[9] A.E. Dwight, in: Proceedings of the 12th Rare Earth Research Conference, Colorado, 1 (1976) 486.
[10] R.V. Skolozdra, L.P. Romaka, L.G. Akselrud, J. Pierre, in: 12th International Conference on Solid Compound of Transition Elements, St Malo, April, 1997.
[11] M.L. Fornasini, R. Marazza, D. Mazzone, P. Riani, G. Zanicchi, Z. Kristallogr. 213 (1998) 108.
[12] Y.D. Seropegin, A.V. Gribanov, O.I. Bodak, in: 12th International Conference on Solid Compound of Transition Elements, St Malo, April, 1997.
[13] L.P. Komarovskaya, R.V. Skolozdra, Izvestlya Akad. Nauk. SSSR Metally 4 (1989) 209.
[14] R.V. Skolozdra, L.P. Komarovs'ka, Soviet Physics-Crystallography, Translated from Kristallografiya 26 (3) (1981) 272.
[15] E. Cordruwisch, H. Noël, P. Boulet, P. Rogl, Journées des Actinides, Uppsala, Sweden, 1998.
[16] C.K. Fair, in: Molen user's manual. An Interactive Intelligent System for Crystal Structure Analysis, Delft, Netherlands, 1989.
[17] D.E. Sands, Q.C. Johnson, O.H. Hikorian, K.L. Kromholtz, Acta Crystallogr. 15 (1962) 1191.
[18] A. Palenzona, J. Less-Common Met. 25 (1971) 367.
[19] A.C. Larson, D.T. Cromer, Acta Crystallogr. 27B (1971) 1875.
[20] F. Steglich, J. Aarts, C.D. Bredl, W. Lieke, D. Meschede, W. Franz, H. Schäfer, Phys. Rev. Lett. 43 (1979) 1892.
[21] T.T.M. Palstra, A.A. Menovsky, J. Van Den Berg, A.J. Dirkmaat, P.H. Kes, G.J. Nieuwenhuys, J.A. Mydosh, Phys. Rev. Lett. 55 (1985) 2727.
[22] M. Lenkewitz, S. Corsepius, G.R. Stewart, J. Alloys Comp. 241 (1996) 121.
[23] P. Boulet, M. Potel, J.C. Levet, H. Noël, J. Alloys Comp. 262–263 (1997) 229.
[24] P. Boulet, H. Noël, Solid State Commun. 107 (3) (1998) 135.
[25] K.H.J. Buschow (Ed.), Handbook of Magnetic Materials, Vol. 6, North Holland, Amsterdam, 1991, p. 85.
[26] F. Weitzer, K. Hiebl, P. Rogl, J. Less-Common Met. 175 (1991) 331.
[27] W. Rieger, E. Parthé, Monatsh. Chemie 99 (1968) 291.